NASA

Technical Memorandum 79544

The Influence of Tortuosity on the Spectrum of Radiation from Lightning Return Strokes

David M. Le Vine

MAY 1978

National Aeronautics and Space Administration

Goddard Space Flight Center
Greenbelt, Maryland 20771

TM 79544

THE INFLUENCE OF TORTUOSITY ON THE SPECTRUM OF RADIATION FROM LIGHTNING RETURN STROKES

David M. Le Vine

May 1978

GODDARD SPACE FLIGHT CENTER
Greenbelt, Maryland

CONTENTS

ILLUSTRATIONS

THE INFLUENCE OF TORTUOSITY ON THE SPECTRUM OF RADIATION FROM LIGHTNING RETURN STROKES

David M. Le Vine

ABSTRACT

An investigation has been made of the influence of tortuosity on the spectrum of radiation from lightning return strokes. The shape of the spectrum obtained by including effects of tortuousity is in keeping with data: The spectrum has a peak in the correct frequency regime followed by an initial decrease as the inverse of frequency. This spectrum is in better agreement with data than the spectrum predicted by the same model without tortuousity (i.e. the long straight channel), which decays at a rate proportional to $1/\nu^2$.

These conclusions were derived from a piecewise-linear "transmission line" model for the channel using in one case simplifying assumptions to arrive at closed form expressions for the spectrum and also from numerical calculations on simulated channels. The analysis indicates an eventual transition to $1/\nu^2$ decrease even for the tortuous channel, which suggests a means for testing the model and gaining insight into return stroke current and channel parameters.

THE INFLUENCE OF TORTUOSITY ON THE SPECTRUM OF RF RADIATION FROM LIGHTNING

INTRODUCTION

Knowledge of the spectrum of radiation from lightning is important both for understanding the dynamics of the lightning flash as well as for assessing the RF interference environment during thunderstorms. Spectral measurements have been reported from frequencies of a few kilohertz (Horner, 1961; Taylor, 1963; Watt and Maxwell, 1957) to frequencies near a GHz (Kosarev, et al., 1970; Hewitt, 1957) and several composite spectra have been deduced from these data by reducing the independent measurements to common units of distance and bandwidth (Horner and Bradley, 1964; Kimpara, 1965; Oh, 1969; Cianos, Oetzel and Pierce, 1972; Oetzel and Pierce, 1969). These composite spectra have several features in common: It is generally agreed that the spectrum peaks near 10 kHz and then decreases roughly inversely with frequency (i.e. as $1/\nu$) upto several hundred MHz. At higher frequencies the data is more scattered: Kimpara (Kimpara, 1965) extrapolates the $1/\nu$ dependence to higher frequencies whereas Oh (Oh, 1969) infers from the data a change from $1/\nu$ to a decrease as approximately $1/\nu^2$ in the decade between 100 MHz and 1 GHz. Representative data are shown in Figure 1.

Theory to rationalize these observations with contemporary best information on lightning parameters have been less widely reported; and in fact, the measurements pose some problems for the modeller. For example, using as a return stroke model a long straight channel (current filament) driven by a current pulse whose shape is consistent with measurements, such as the paired exponentials of the Bruce-Golde form or as modified to include continuing current (Bruce-Golde, 1941; Uman, 1969; Price and Pierce, 1974), and assuming

that the current pulse propagates along the channel with velocity, v (i.e. I(z,t) = I(t-z/v)), one has the "transmission line" model presently in use (Dennis and Pierce, 1964; Uman and McLain, 1969). It is not particularly difficult with this model to calculate the electric field radiated to a distant observer, employing for example the Fraunhoffer approximation (e.g. Le Vine and Meneghini, 1976). Assuming typical channel lengths and velocities of propagation, this calculation yields a spectrum whose peak is in the correct frequency range (tens of kilohertz); however, the high frequency asymptote decays as $1/\nu^2$, not inversely with the first power of frequency as the data suggests.

It is the purpose of this paper to show that by introducing tortuosity into the channel model – that is, using the transmission line model but allowing the channel to be irregular rather than straight – one obtains a spectral decay proportional to $1/\nu$. The spectrum obtained with tortuousity included also peaks near 10 kHz, and then decreases roughly as $1/\nu$ until, at an upper frequency determined by the scale of tortuousity, it begins to decrease as $1/\nu^2$. The shape is similar to that reported by Oh (Oh, 1969).

Relatively little attention has been devoted to the effects of tortuousity on the fields radiated from lightning return strokes. Hill (Hill, 1969) has treated the subject using a scalar analysis based on the moment approximation and the Bruce-Golde form for motion along the channel. This restricts the analysis to VLF (for which it was intended). On the other hand, at frequencies of 10 MHz or so, the free space wavelength of the radiated fields is comparable to the typical step size (the channel is formed in discrete pieces during the stepped leader processes; Uman, 1969) and the individual elements of which the channel is formed may become effective radiators. In this paper, the effects of tortuousity are analyzed by adopting a piecewise linear model for the channel and assuming that the

current pulse propagates along the channel with constant velocity on each segment: $\bar{J}(r,t) = \hat{\ell}\, f(t-\hat{\ell}\cdot\bar{r}/v)$. This is the "transmission line" model applied on a piecewise basis to the channel. Both an analytical model for the spectrum, based on simplifying assumptions, and numerical results will be presented. The numerical results are obtained by having a computer produce channel realizations in accordance with pre-assigned statistics for mean length and orientation of individual elements. Then the spectrum is computed for each realization using formulas for the radiation from each individual element keeping track of the phase as the current pulse propagates up the channel (Le Vine and Meneghini, 1978b). The analytical results are obtained by simplifying the expressions for radiation from each element sufficiently that sums and averages can be performed explicitly. The results agree.

MODEL

Consider a filament L units long in the $\hat{\ell}$ direction driven by the traveling current wave:

$$\bar{J}(\bar{r},t) = \hat{\ell}\, f(t-\hat{\ell}\cdot\bar{r}/v)$$

where v is the velocity of propagation along the channel, and assume that the filament is arbitrarily oriented above a conducting plane at z = 0.

One can obtain a solution for the fields produced by such a current filament by transforming to the frequency domain and solving in terms of potentials. Doing so, one obtains the following form for the magnetic vector potential:

$$\tilde{\bar{A}}(\bar{r}_o, \nu) = \mu\, \tilde{f}(\nu) \int_{\text{filament}} e^{jk\eta\hat{\ell}\cdot\bar{r}_s} \left\{ \hat{\ell}\, \frac{e^{jkR}}{4\pi R} + \hat{\ell}'\, \frac{e^{jkR'}}{4\pi R'} \right\} d\bar{r}_s \qquad (1)$$

where the superscript tilda (~) denotes a Fourier transform (for example, $\tilde{f}(\nu)$ is the Fourier transform of f(t)) and where $R = |\bar{r}_o - \bar{r}_s|$ is the distance from the source point $\bar{r}_s$ to the observer $\bar{r}_o$ and $R' = |\bar{r}_o - \bar{r}_s'|$ is the distance from the image source point $\bar{r}_s' = \bar{r}_s - 2\hat{z}(\bar{r}_s\cdot\hat{z})$ to the observer, and $\hat{\ell}' = \hat{\ell} - 2\hat{z}(\hat{\ell}\cdot\hat{z})$ and $\eta = c/v$. The electromagnetic fields are obtained from Equation 1 by means of the formulas:

$$\tilde{\bar{E}}(\bar{r}_o, \nu) = jkc \left[\tilde{\bar{A}}(\bar{r}_o, \nu) + \frac{1}{k^2} \nabla (\nabla\cdot\tilde{\bar{A}}) \right] \qquad (2a)$$

$$\tilde{\bar{H}}(\bar{r}_o, \nu) = \frac{1}{\mu} \nabla\cdot\tilde{\bar{A}} \qquad (2b)$$

In general, the integral in Equation 1 can not be evaluated and approximations must be made. The Fraunhoffer approximation (i.e. far field approximation) will be employed here. (In the special case v = c the integral can be evaluated exactly in closed form (Le Vine and Meneghini, 1978a; Schelkunoff, 1952); although for real lightning, v < c, and

generally v is not even constant along the channel.) To obtain the Fraunhoffer approximation, Equation 1 is substituted into Equation 2 and it is assumed that the filament length, L, is smaller than the distance, R, from filament to observer. Then a Taylor series expansion is made of R about the filament center at $\bar{r}_c$. Letting $\rho_c = |\bar{r}_0 - \bar{r}_c|$ and assuming that $L/\rho_c < 1$, $kL^2/\rho_c \ll 2\pi$, $k\rho_c \gg 1$ and keeping only lowest order terms in $k\rho_c$, one obtains the following form for the radiated fields:

$$\bar{E}(\bar{r}_o, \nu) = \sqrt{\mu/\epsilon}\ \tilde{f}(\nu) \left\{ [\hat{\ell} - (\hat{\ell}\cdot\nabla\rho_c)\nabla\rho_c] \frac{e^{jk\rho_c}}{4\pi\rho_c}\ I(\nu) - [\hat{\ell}' - (\hat{\ell}'\cdot\nabla\rho_c)\nabla\rho_c'] \frac{e^{jk\rho_c'}}{4\pi\rho_c'}\ I'(\nu) \right\} \tag{3a}$$

$$\tilde{\bar{H}}(\bar{r}_o, \nu) = \tilde{f}(\nu) \left\{ (\nabla\rho_c \times \hat{\ell}) \frac{e^{jk\rho_c}}{4\pi\rho_c}\ I(\nu) - (\nabla\rho_c' \times \hat{\ell}') \frac{e^{jk\rho_c'}}{4\pi\rho_c'}\ I'(\nu) \right\} \tag{3b}$$

where

$$I(\nu) = e^{jk\eta(\hat{\ell}\cdot\bar{r}_c)} \left[\frac{e^{j\frac{1}{2}kL(\eta-\hat{\ell}\cdot\nabla\rho_c)} - e^{-j\frac{1}{2}kL(\eta-\hat{\ell}\cdot\nabla\rho_c)}}{\eta - \hat{\ell}\cdot\nabla\rho_c} \right]$$
$$= jkL\ e^{jk\eta(\hat{\ell}\cdot\bar{r}_c)}\ \mathrm{sinc}\ [\tfrac{1}{2}kL(\eta-\hat{\ell}\cdot\nabla\rho_c)] \tag{4a}$$

$$I'(\nu) = e^{jk\eta(\hat{\ell}'\cdot\bar{r}_c')} \left[\frac{e^{j\frac{1}{2}kL(\eta-\hat{\ell}'\cdot\nabla\rho_c')} - e^{-j\frac{1}{2}kL(\eta-\hat{\ell}'\cdot\nabla\rho_c')}}{\eta - \hat{\ell}'\cdot\nabla\rho_c'} \right]$$
$$= jkL\ e^{jk\eta(\hat{\ell}'\cdot\bar{r}_c')}\ \mathrm{sinc}\ [\tfrac{1}{2}kL(\eta-\hat{\ell}'\cdot\nabla\rho_c')] \tag{4b}$$

An interesting interpretation of Equations 3 and 4 is obtained by noting that the phase terms (the arguments of the exponentials) can be written in the form $j2\pi\nu\tau$ where $\tau = (\rho_c/c - \hat{\ell}\cdot\bar{r}_c/\nu) \pm \frac{1}{2}(L/\nu - L/c\ \hat{\ell}\cdot\nabla\rho_c)$. The first term in parenthesis is just the time required for a signal to propagate from the filament center to the observer plus an arbitrary constant $(\hat{\ell}\cdot\bar{r}_c/\nu)$ which is necessary if several elements are to be compared. The

remaining parenthesis is the binomial correction of this time corresponding to propagation from the upper and lower ends of the filament ($\pm \frac{1}{2c} \hat{\mathbf{r}} \cdot \nabla \rho_c$) plus the time required for the pulse to propagate from one end of the filament to the other (L/v). That is, within the limitations of the Fraunhoffer approximation the radiation may be regarded as consisting of two pulses which emanate from the ends of the filament but with a relative delay equal to the time required for the pulse to propagate the length of the filament. Interestingly, this is exactly what one finds to be true for the exact solution when v = c (Le Vine and Meneghini, 1978a).

Associating the radiation with the end points of the filament permits a simple interpretation of effects of tortuosity. When the current pulse begins to propagate up the filament, a pulse of radiation (having the shape of the current pulse) is radiated from the bottom of the filament, and nothing more happens until the current pulse reaches the top of the filament; then an identical pulse, but of opposite sign, is emitted and the total radiation is now the sum of these two terms (Uman, McLain & Krider, 1975; Le Vine & Meneghini, 1978a). If one now joins several segments together to form a long channel, then the radiation is associated with the junction points (top of one filament and bottom of the adjoining filament), and the composite channel radiates from its "kinks". The tortuous channel is one with many kinks, and therefore has many sources of radiation. As a result there is the potential for more structure (i.e. variability) in the signal radiated from the tortuous channel than from the long straight channel which radiates only from its two ends. Consequently, one would expect that the spectrum of the tortuous channel will have its high frequency power increased in comparison with the equivalent straight channel, a conclusion which is supported by the analysis and examples to be presented below.

Within the limitations inherent in the Fraunhoffer approximation, either the "kink" picture or the more conventional interpretation which associates radiations with the filament center, yield equivalent results. Which picture one adopts depends on which of the two forms is adopted for $I(\nu)$ in Equation 4. For purposes of the analysis to follow, radiation will be associated with the filament center; however, in the computer simulation it was more convenient to separate the two exponentials in the sinc(x) function.

ANALYSIS

Mathematically the radiation seen by an observer appears to be a sequence of pulses emitted from each element with a temporal history dependent on the manner in which the pulse propagates up the channel and on the nature (length and orientation) of the individual elements of which the channel is comprised. Associating these pulses with the filament center, the electric field emitted from the n-th element as seen by an observer (for simplicity) on the surface is obtained from Equation 3:

$$\tilde{\bar{E}}_n(\bar{r},\nu) \cong j\frac{\sqrt{\mu/\epsilon}}{\pi\eta}\,\tilde{f}(\nu)\,a_n \sin(\tfrac{1}{2}k\eta L_n)\,e^{jkc\tau_n} \tag{5}$$

where

$$a_n = \frac{\hat{e}_n(\rho_{c_n})\cdot\hat{z}}{\rho_{c_n}} \tag{6a}$$

$$\tau_n = \frac{1}{c}\left\{\rho_{c_n} + \eta\sum_{s=1}^{n}\tfrac{1}{2}[L_{s-1}+L_s]\right\} \tag{6b}$$

where L_n is the length of the n-th element and in order to simplify the algebra, it has been assumed that $\hat{\ell}_n \cdot \nabla\rho_{c_n} \ll \eta$. The total field, $\tilde{E}(\bar{r},\nu)$, seen by the observer is the sum over all n of the $\tilde{E}_n(\bar{r},\nu)$, and the spectrum of this radiation is defined to be:

$$S(\nu) \triangleq \sqrt{\langle\tilde{E}(\bar{r},\nu)\,\tilde{E}^*(\bar{r},\nu)\rangle}$$

where the pointed brackets $\langle\ \rangle$ denote a statistical average. Using Equation 5, one obtains the following form for the spectrum:

$$\tilde{E}(\bar{r},\nu)\,\tilde{E}^{*}(\bar{r},\nu) = \left[\frac{\sqrt{\mu/\epsilon}}{\pi\eta}\,|\tilde{f}(\nu)|\right]^{2}\left\{\sum_{\text{all } n} a_n \sin(\tfrac{1}{2}k\eta L_n)e^{jkc\tau_n}\right\}\cdot\left\{\sum_{\text{all } m} a_m \sin(\tfrac{1}{2}k\eta L_m)e^{-jkc\tau_m}\right\} \tag{7}$$

$$= \left[\frac{\sqrt{\mu/\epsilon}}{\pi\eta}\,|\tilde{f}(\nu)|\right]^{2}\sum_{\substack{\text{all } n\\ \text{all } m}} a_n a_m \sin(\tfrac{1}{2}k\eta L_n)\sin(\tfrac{1}{2}k\eta L_n)e^{jkc[\tau_n-\tau_m]}$$

In order to perform the required averages assume that: 1) The a_n, L_n and τ_n are independent random variables; 2) The phase $kc(\tau_n-\tau_m)$ is uniformly distributed over 2π; and 3) $\rho_{c_n} \cong \rho_c$ where ρ_c is a constant, so that the a_n may be assumed to be identically distributed. Then, the diagonal terms in the sum are dominant (e.g. Kodis, 1966) and one obtains:

$$\langle\tilde{E}(\bar{r},\nu)\,\tilde{E}^{*}(\bar{r},\nu)\rangle \cong \left[\frac{\sqrt{\mu/\epsilon}}{\pi\eta}\,|\tilde{f}(\nu)|\right]^{2} N\langle a_n^{2}\rangle\langle\sin^{2}(\tfrac{1}{2}k\eta L_n)\rangle \tag{8}$$

where N is the number of elements in the channel. In order to perform the average over the element lengths, L_n, it will be assumed that the L_n are exponentially distributed with mean L_0. Based on observations of stepped leaders one would expect L_0 to be on the order of several 10's of meters (Uman, 1969; Schonland, 1956); however, little information exists concerning the actual statistics of the L_n. Fortunately, the limiting behavior of the average at high and low frequencies, which is the important factor for the discussion to follow, is independent of the choice of the distribution (Appendix A) and so the conclusions may be representative even if the assumed distribution is not. Also, the numerical results to be presented later support the conclusions reached here, but do not assume exponentially distributed L_n. Performing the average over the L_n in equation 8, one obtains:

$$\langle\sin^{2}(\tfrac{1}{2}k\eta L_n)\rangle = \tfrac{1}{2}\,\frac{(k\eta L_0)^{2}}{1+(k\eta L_0)^{2}} \tag{9}$$

Employing this result in Equation 8, one obtains the following form for the spectrum of radiation from the tortuous channel:

$$S(\nu) = S_0 \left[\frac{(k\eta L_0)^2}{1+(k\eta L_0)^2} \right]^{\frac{1}{2}} |\tilde{f}(\nu)| \qquad (10)$$

where

$$S_0 = \frac{\sqrt{\mu/\epsilon}}{\pi\eta\rho_c} [\tfrac{1}{2}N\langle a_n^2\rangle]^{\frac{1}{2}}$$

Notice that at high frequencies ($k\eta L_0 \gg 1$), $S(\nu)$ is proportional to $|\tilde{f}(\nu)|$ and that at low frequencies ($k\eta L_0 \ll 1$), $S(\nu)$ is proportional to $\nu|\tilde{f}(\nu)|$. That is, in the high frequency limit, the spectrum of radiated electric field is proportional to the spectrum of the current pulse, whereas in the low frequency limit it is proportional to the spectrum of the current pulse multiplied by frequency. The definition of low frequency must be treated carefully here because for low enough frequency the assumptions inherent in the Fraunhoffer approximation fail and the analysis is not correct. More precisely, the low frequency behavior of $S(\nu)$ is to be regarded as the shape of the spectrum in an intermediate frequency range between (roughly) $k\eta L_0 = 1$ and the low frequency bound on the Fraunhoffer approximation, roughly at $k\rho_c = 1$. In this intermediate range $S(\nu)$ is proportional to $\nu|\tilde{f}(\nu)|$ and at high frequencies $S(\nu)$ is proportional to $|\tilde{f}(\nu)|$.

To appreciate the significance of these two regions, and to compare with data, the form of the current pulse is required. A pulse shape representative of currents measured in lightning return strokes is:

$$I(t) = I_1 [e^{-\alpha t} - e^{-\beta t}] + I_2 [e^{-\gamma t} - e^{-\delta t}] \qquad (11)$$

where for typical first return strokes $\alpha = 2 \times 10^4$, $\beta = 8 \times 10^5$, $\gamma = 10^3$ and $\delta = 2 \times 10^4$, and $I_1 = 30$ kA and $I_2 = 2.5$ kA. The shape of this current pulse is shown at the top in Figure 2 (and its spectrum $|\tilde{f}(\nu)|$ is plotted at the bottom). The first two exponentials in this expression represent the main current pulse in a form proposed by Bruce and Golde (1941) with parameters suggested by Dennis and Pierce (1964). The third term, $I_2 \exp(-\gamma t)$, represents intermediate current (Uman, 1969); and the remaining exponential, $I_2 \exp(-\delta t)$, has been added to achieve continuity at $t = 0$ and doesn't, otherwise, significantly alter the current pulse. Details of the propagation of current during return strokes are still at issue (e.g., Price and Pierce, 1977). However, the preceding waveform reasonably represents a composite of reported current measurements (Uman, 1969; Dennis and Pierce, 1964).

The Fourier transform of the pulse given in Equation 11 is:

$$\tilde{f}(\nu) = \frac{I_0}{(2\pi\nu)^2} \left\{ \frac{\beta - \alpha}{[1 + j\frac{\alpha}{2\pi\nu}][1 + j\frac{\beta}{2\pi\nu}]} + \frac{I_1}{I_0} \frac{\delta - \gamma}{[1 + j\frac{\gamma}{2\pi\nu}][1 + j\frac{\delta}{2\pi\nu}]} \right\} \quad (12)$$

$|\tilde{f}(\nu)|$ is plotted in Figure 2 (bottom) for the parameters listed above. Notice in particular, that in the limit of large frequency ($\nu >> \beta/2\pi$), the function $|\tilde{f}(\nu)|$ decreases as $1/\nu^2$, and that $|\tilde{f}(\nu)|$ is constant in the low frequency limit.

Now substituting Equation 12 for $|\tilde{f}(\nu)|$ into Equation 10, one can examine the high and "low" frequency behavior of the spectrum. Since the spectrum $S(\nu)$ of the radiated fields is proportional to $|\tilde{f}(\nu)|$ in the high frequency limit, $S(\nu)$ decreases as $1/\nu^2$ at high enough frequencies independent of tortuousity. However, at intermediate frequencies – large enough that $\nu > \beta/2\pi$ but small enough $k\eta L_0 < 1$ – the spectrum $S(\nu)$ is proportional to $\nu|\tilde{f}(\nu)|$ and therefore decreases only as $1/\nu$. This slower rate of decrease at intermediate frequencies is a direct consequence of tortuousity. In contrast, the spectrum of a

single straight channel (no tortuousity) does not exhibit an intermediate region with $1/\nu$ decrease but rather reaches a peak and then rolls off as $|\tilde{f}(\nu)|$ which is to say as $1/\nu^2$ (Le Vine and Meneghini, 1976). Existence of the intermediate region for the tortuous channel is consistent with available information on lightning return strokes. For example, letting $L_0 = 30$ meters, which is typical of the length of steps during the stepped leader (Uman, 1969), and letting $\eta = 3$ which is reasonable for return stroke velocities (Uman, 1969), one obtains $k\eta L_0 = 1$ at $\nu = 0.5$ MHz but with $\beta = 8 \times 10^5$, $|\tilde{f}(\nu)|$ has already begun to decrease as $1/\nu^2$ at these frequencies.

This section has demonstrated how randomness of the channel can introduce energy at intermediate frequencies and thereby slow the rate of decrease of the spectrum. Examples and a comparison with experiment will be presented in the following section where it will be shown that this effect is consistent with data.

EXAMPLES

In this section the effects of tortuousity will be illustrated with spectra calculated from simulated lightning channels. A simulation for the purpose of studying the effects of tortuousity has been developed by this author and a colleague (R. Meneghini) using a piecewise linear model for the channel and employing Equations 3 and 4 for the fields radiated from each element (Le Vine and Meneghini, 1978b). In this simulation the channel is generated by placing end-to-end linear segments chosen by the machine in accordance with assigned statistics. The procedure is suggestive of real cloud-to-ground lightning in which the channel is formed in a series of discrete steps called the stepped leader. In fact, the simulation has been written so that radiation from the stepped leader may also be studied. In most of the work done to date, the channel elements were chosen by assuming that the change in the (cartesian) coordinates required to advance from one end point to the next of a given element were normally distributed. Typically, the x- and y-coordinates were identically distributed with zero mean and the z-coordinate had non-zero mean and a standard deviation on the order of 20 meters. Obviously, one can control the general direction of the channel through choice of the mean value of the coordinate change, and can control the variations about this direction by means of the assigned standard deviations. Typical element lengths in the channels used here were 40 meters, but have ranged from about 30 meters to 300 meters. Figure 3 shows a channel generated by the computer, in this case without branches. (The simulation is three dimensional so the projection of the channel on orthogonal planes is shown.) Once the channel has been generated, the computer calculates both the temporal history of the electromagnetic fields produced by a current pulse propagating

along this channel and also the manitude of the Fourier transform (spectrum) of the radiated waveform. This is done using the solutions given in Equations 3 and 4 and their time domain equivalent, and employing an assigned current waveform such as given in Equation 11. The major computational problem is keeping track of the proper phase of the current in each of the many elements which may be radiating at a given instant. (See Le Vine and Meneghini, 1978b for examples and a comparison in the time domain of simulated waveforms with data.)

The influence of tortuousity on the spectrum of the radiated fields is illustrated in Figure 4. For comparison sake, the envelope of the spectrum, $S(\nu)$, is plotted for both a long straight channel (no tortuousity) and an equivalent tortuous channel. The current waveform given in Equation 11 was used with a velocity of propagation of $v = c/2$ in both cases. The tortuous channel used in this calculation is shown in Figure 3, and was generated from segments whose mean length was about 40 meters with variance of each cartesian coordinate of about 20 meters. In this example, the observer is 50 km away and is located on the conducting surface. The length of the vertical channel (about 5 km) was chosen so that its spectral peak was nearly identical with that of the tortuous channel. This was done to facilitate comparison of shapes of the two spectra. [See Le Vine and Meneghini (1976) for a discription of the effects of other parameters such as channel length and orientation, and velocity of propagation on the spectrum of the straight channel.]

Both spectra shown in Figure 4 peak near 10 kHz, but the spectrum associated with the straight channel falls off at high frequencies as $1/\nu^2$ whereas the spectrum associated with the tortuous channel decreases more slowly, first roughly as $1/\nu$, and then near about 3 MHz begins to decrease as $1/\nu^2$. The high frequency asymptote in both cases is determined by the current waveform (as discussed above) and therefore should be $1/\nu^2$; however,

the variability introduced by tortuousity introduces additional energy at intermediate frequencies slowing the rate of decrease of the spectrum in this frequency regime. These spectra have the shape deduced from the analysis of the preceding section.

The spectrum associated with the tortuous channel is consistent with measured spectra. This is illustrated in Figure 5 where representative data (Kimpara, 1965) have been plotted with the calculated spectra shown in Figure 4. (The data points were obtained from Figure 1 of Kimpara, 1965, and normalized to unit bandwidth and an observer 50 km from the channel.) As can be seen the spectrum associated with the tortuous channel (solid line) has a shape consistent with the data at intermediate frequencies; in contrast, the spectrum of the equivalent straight channel falls off too rapidly to agree well with the data. Eventually, at a frequency determined by the mean length of the elements in the channel, the spectrum computed from the tortuous channel also begins to decrease as $1/\nu^2$. The transition from $1/\nu$ to $1/\nu^2$ decay is not inconsistent with data at high frequencies (e.g. Pierce, 1977) and in fact Oh (Oh, 1969) interprets the data to have such a transition, although in the vicinity of 100 MHz. If confirmed by measurements, such a transition would have important implications. First, establishing the frequency regime in which the transition occurs would provide a measure of the scale of channel tortuousity (i.e. the mean element length) and by inference of the step length in the stepped leader. Secondly, establishing the rate of decrease of the spectrum at frequencies beyond the transition would yield insight into the shape of the current pulse because in this regime the spectrum is dominated by the pulse shape. Certainly, if a transition to $1/\nu^2$ were to be found in the data, it would support the transmission line model and the current waveform in most common use (Equation 10).

SUMMARY

The general shape of the spectrum obtained by including effects of tortuousity is in keeping with data: It predicts a peak in the correct frequency regime followed by a decrease as the inverse of frequency, which persists to a frequency dependent on the length of the elements in the channel. This spectrum is in better agreement with data than the spectrum predicted by the same model without tortuousity (i.e. the long straight channel), which decays at a rate proportional to $1/\nu^2$.

These conclusions were derived from a piecewise-linear "transmission line" model for the channel both using simplifying assumptions to arrive at closed form expressions for the spectrum and from numerical calculations on simulated channels. The analysis suggests an eventual transition to $1/\nu^2$ decrease even for the tortuous channel, which suggests a potential means for testing the model and gaining insight into return stroke current and channel parameters.

REFERENCES

Bruce, C. E. R. and R. H. Golde (1941), "The Lightning Discharge", JIEE (London), Vol. 88 (II), pp. 487-505.

Cianos, N., G. N. Oetzel and E. T. Pierce (1972), "Structure of Lightning Noise – Especially above HF", Lightning and Static Electricity Conference, December, Wright Patterson AFB.

Churchill, R. V. (1969), Fourier Series and Boundary Value Problems, 2nd Ed., McGraw-Hill, p. 87.

Dennis, A. S. and E. T. Pierce (1964), "The Return Stroke of the Lightning Flash to Earth as a Source of VLF Atmospherics", Radio Science Vol. 68D(7), pp. 777-794.

Hewitt, F. J. (1957), "Radar Echos from Intra-Stroke Processes in Lightning", Proc. Phys. Soc. (London), Vol. 70(B), pp. 961-979.

Hill, R. D. (1969), "Electromagnetic Radiation from Erratic Paths of Lightning Strokes", J. Geophys. Res., Vol. 74(8), pp. 1922-1929.

Horner, F. (1961), "Narrow Band Atmospherics from Two Local Thunderstorms", J. Atmos. Terr. Phys., Vol. 21, pp. 13-25.

Horner, F. and P. A. Bradley (1964), "The Spectra of Atmospherics from Near Lightning Discharges", J. Atmos. Terr. Phys., Vol. 26, pp. 1155-1166.

Kaplan, W. (1952), Advanced Calculus, Addison-Wesley, Chapt. 6.

Kimpara, A. (1965), "Electromagnetic Energy Radiated from Lightning", in Problems in Atmospheric and Space Electricity, S. C. Coroniti, Ed., Elsevier Pub. Co., pp. 352-365.

Kodis, R. D. (1966), "A Note on the Theory of Scattering from an Irregular Surface", IEEE Trans. Vol. AP-14(1), pp. 77-82.

Kosarev, E. L., V. G. Zatsepin and A. V. Mitrofanov (1970), "Ultrahigh Frequency Radiation from Lightning", J. Geophys. Res., Vol. 75(36), pp. 7524-7530.

Le Vine, D. M. and R. Meneghini (1976), "Radiation from a Current Filament Driven by a Traveling Wave", NASA TN-D-8302, Available from NTIS #N77-1129.

Le Vine, D. M. and R. Meneghini (1978a), "Electromagnetic Fields Radiated from a Lightning Return Stroke: Application of an Exact Solution to Maxwell's Equations", J. Geophys. Res., Vol. 83, (NC5), pp. 2377-2384.

Le Vine, D. M. and R. Meneghini (1978b), "Simulations of Radiation from Lightning Return Strokes: The Effects of Tortuousity", Radio Science, Vol. 6. Oct.

Oetzel, G. N. and E. T. Pierce (1969), "Radio Emissions from Close Lightning", in Planetary Electrodynamics, Vol. 1, S. C. Coroniti and J. Hughes, Ed., Gredon and Breach, N.Y., pp. 543-569.

Oh, L. L. (1969), "Measured and Calculated Spectral Amplitude Distribution of Lightning Sferics", IEEE Trans., Vol EMC-11 (4), pp. 125-130.

Pierce, E. T. (1977), "Atmospherics and Radio Noise", Chap. 10 of Lightning, Vol. 1, Academic Press, R. A. Golde, Ed.

Price, G. H. and E. T. Pierce (1977), "The Modelling of Channel Current in the Lightning Return Stroke", Radio Science, Vol. 12(3), pp. 381-388.

Schelkunoff, S. A. (1952), Advanced Antenna Theory, John Wiley and sons, New York, pp. 102-109.

Schonhand, B. F. J. (1956), "The Lightning Discharge", Encyclopedia of Physics, S. Flugge, Ed., Vol. XXII, pp. 576-628.

Taylor, W. L. (1963), "Radiation Field Characteristics of Lightning Discharges in the Band 1 kc/s to 100 kc/s", J. Res. Nat. Bur. Stand., Vol. 64D, pp. 349-355.

Uman, M. A. (1969), Lightning, McGraw-Hill.

Uman, M. A., D. K. McLain and E. P. Krider, (1975), "The Electromagnetic Radiation from a Finite Antenna", Amer. J. Phys., Vol. 43, pp. 33-38.

Uman, M. A. and D. K. McLain (1969), "Magnetic Field of Lightning Return Stroke", J. Geophys. Res., Vol. 74(28), pp. 6899-6910.

Watt, A. D. and E. L. Maxwell (1957), "Measured Statistical Characteristics of VLF Atmospheric Radio Noise", Proc. IRE, Vol. 45(1), pp. 55-62.

FIGURE CAPTIONS

Figure 1. Summary of spectral measurements from lightning. These data have been normalized to a distance of 50 km and unit bandwidth. The spectrum is proportional to (frequency)$^{-1}$ in the frequency range from a few 10's of kilohertz to about 100 megahertz.

Figure 2. The current pulse used in the calculations and its spectrum (i.e. magnitude of its Fourier transform). The current pulse is representative of current in first return strokes. In this example, $\alpha = 2\delta = 4 \times 10^4$ sec^{-1}; $\beta = 8 \times 10^5$ sec^{-1}; $\gamma = 10^3$ sec^{-1} and $I_0 = 30$ kA and $I_1 = 2.5$ kA.

Figure 3. Example of a tortuous channel produced by the computer simulation.

Figure 4. The spectrum calculated from a straight channel (about 5 km long) and a tortuous channel (the one shown in Figure 3). Only the envelopes of the calculated spectra are plotted. The current pulse shown in Figure 2 was employed assuming a velocity of propagation equal to c/2. The observer is 50 km from the channel.

Figure 5. The calculated spectra (from Figure 4) with representative data points superimposed. The data were taken from Kimpara (Kimpara, 1965) normalized to 50 km and unit bandwidth.

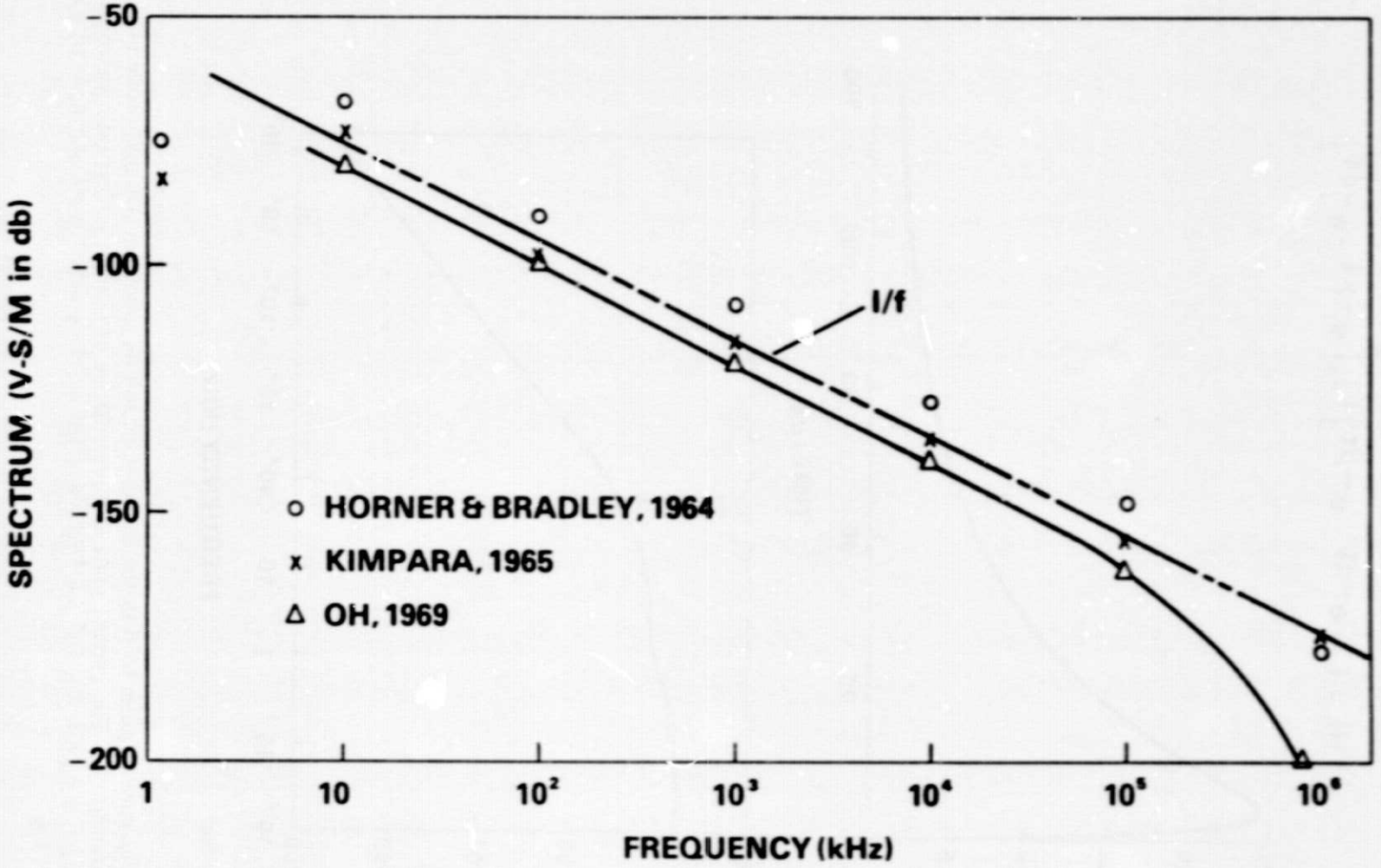

Figure 1: Summary of spectral measurements from lightning. These data have been normalized to a distance of 50 km and unit bandwidth. The spectrum is proportional to (frequency)$^{-1}$ in the frequency range from a few 10's of kilohertz to about 100 megahertz.

$$I(t) = I_0\left[e^{-\alpha t} - e^{-\beta t}\right] + I_1\left[e^{-\gamma t} - e^{-\delta t}\right]$$

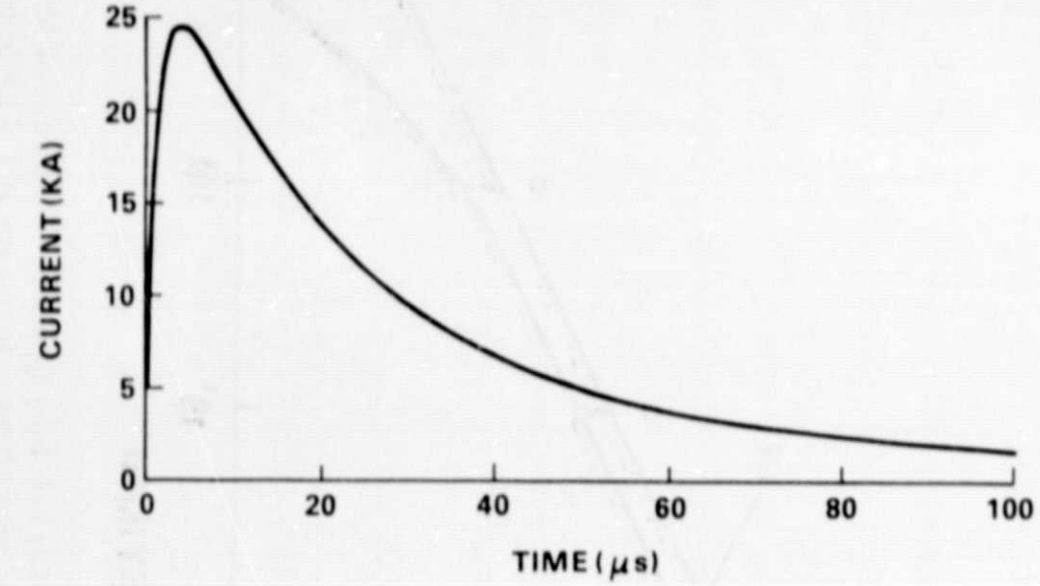

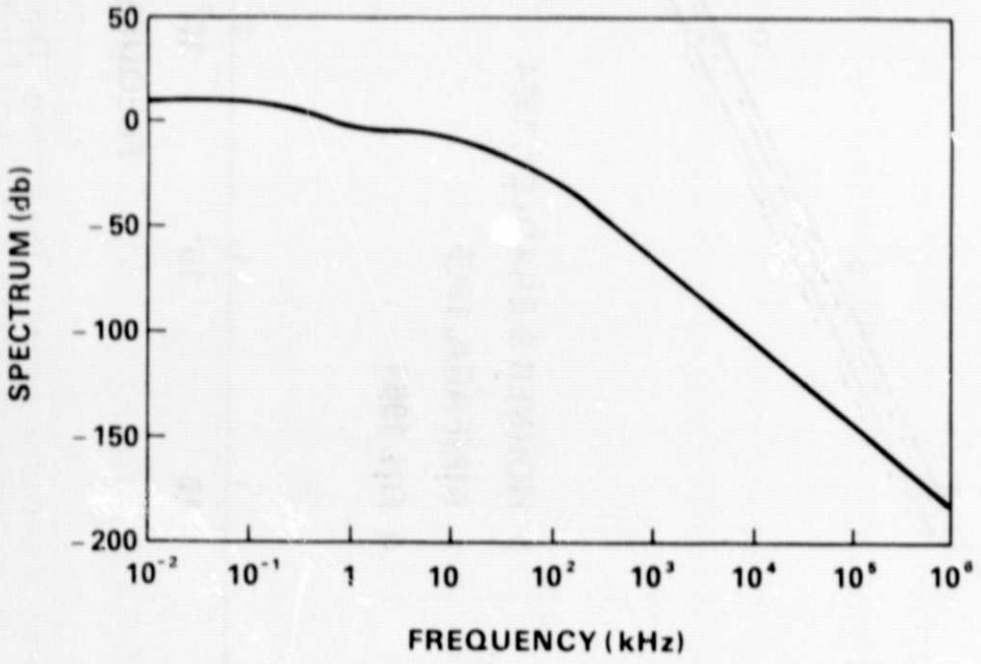

Figure 2: The current pulse used in the calculations and its spectrum (i.e. magnitude of its Fourier transform). The current pulse is representative of current in first return strokes. In this example, $\alpha = 2\delta = 4 \times 10^4$ sec^{-1}; $\beta = 8 \times 10^5$ sec^{-1}; $\gamma = 10^3$ sec^{-1} and $I_0 = 30$ kA and $I_1 = 2.5$ kA.

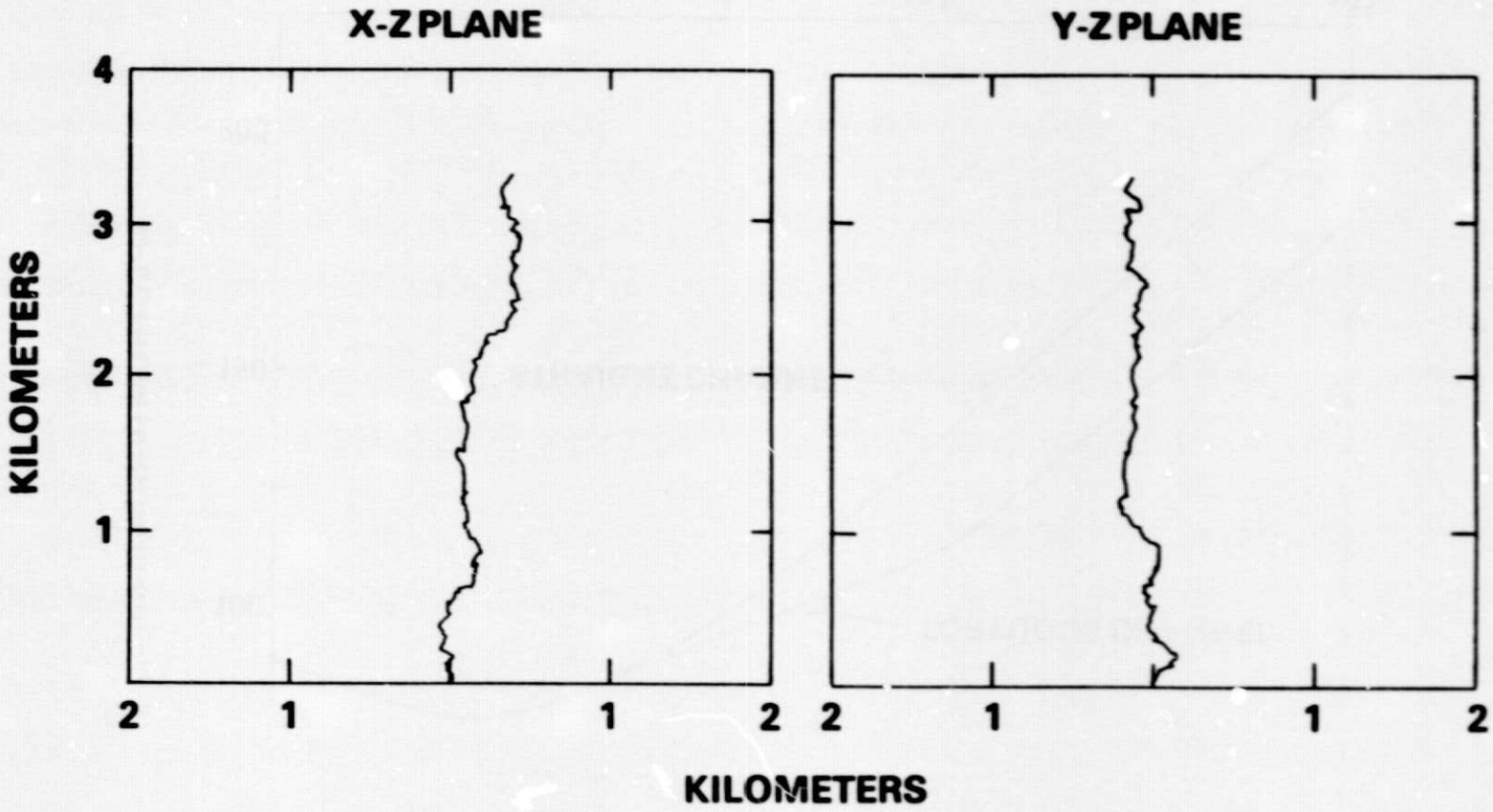

Figure 3. Example of a tortuous channel produced by the computer simulation.

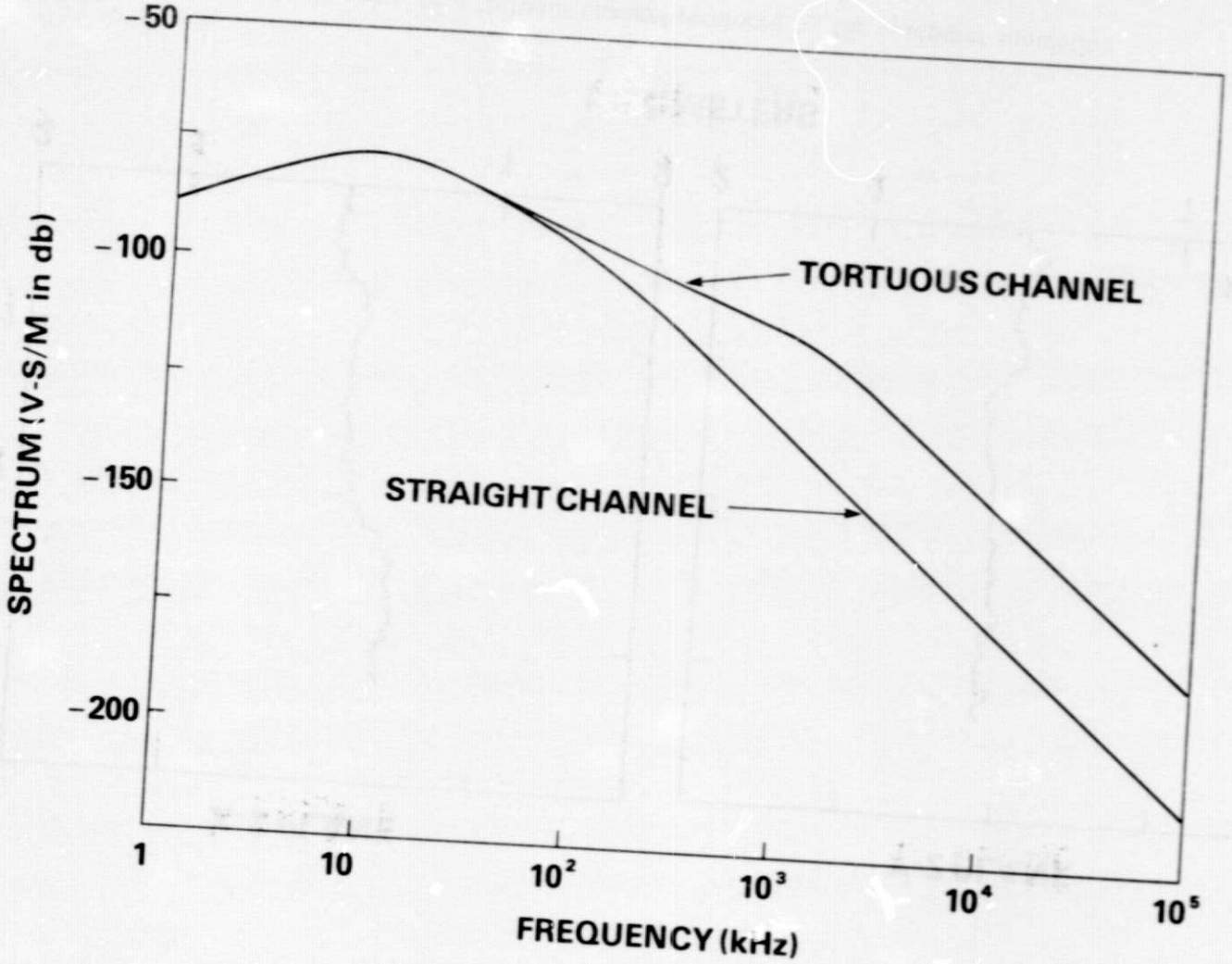

Figure 4. The spectrum calculated from a straight channel (about 5 km long) and a tortuous channel (the one shown in Figure 3). Only the envelopes of the calculated spectra are plotted. The current pulse shown in Figure 2 was employed assuming a velocity of propagation equal to c/2. The observer is 50 km from the channel.

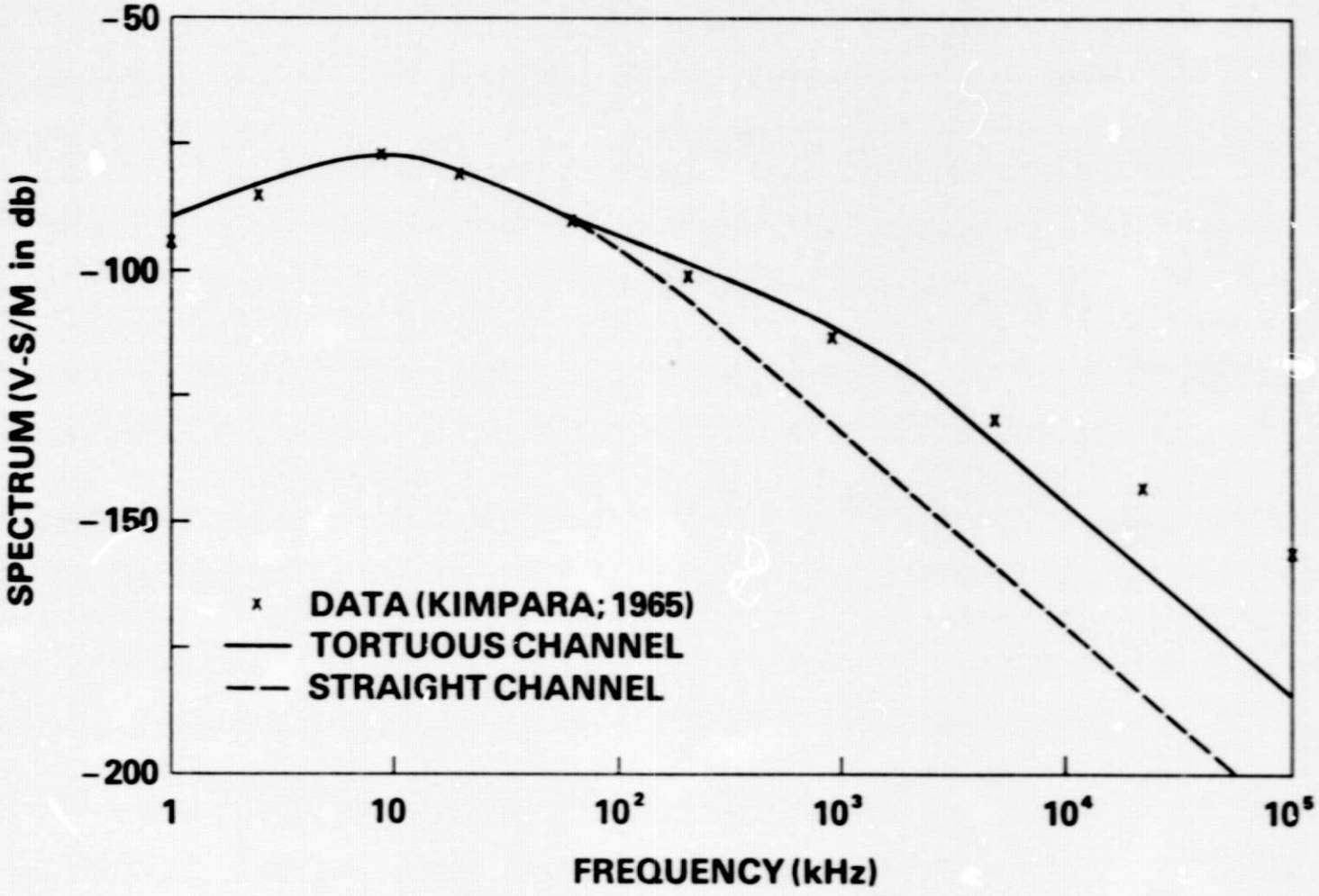

Figure 5. The calculated spectra (from Figure 4) with representative data points superimposed. The data were taken from Kimpara (Kimpara, 1965) normalized to 50 km and unit bandwidth.

APPENDIX A

In this appendix the average $\langle \sin^2(\alpha x) \rangle$ will be performed in the limit of large and small α. It will be shown that the limits are independent of the probability density function, P(x), for a large class of P(x).

A. The large α limit:

$$\langle \sin^2(\alpha x) \rangle = \int_0^\infty P(x) \sin^2(\alpha x) dx$$

which is absolutely convergent because $\int_0^\infty |P(x)| dx = 1$. Now letting $\sin^2(\alpha x) = \frac{1}{2}(1 - \cos 2\alpha x)$, one obtains:

$$\langle \sin^2(\alpha x) \rangle = \frac{1}{2} - \frac{1}{2} \int_0^\infty P(x) \cos(2\alpha x) dx$$

But the integral on the right is zero in the limit $\alpha \to \infty$ for piecewise continuous P(x) (e.g. see the Riemann-Lesbeque theorem, or Churchill, 1969).

B. The small α limit:

From the theory for power series one can write:

$$\sin^2(y) = y^2 + (1 - 2\cos^2\hat{y}) \frac{y^4}{3}$$

where the last term on the right is the remainder after 4 terms of the MacLaurin series for $\sin^2(y)$ and $\hat{y}$ is some particular y chosen to make both sides equal (e.g. Kaplan, 1952). With this result one obtains:

$$\langle \sin^2(\alpha x) \rangle = \alpha^2 \int_0^\infty x^2 P(x)dx + \alpha^4 \int_0^\infty (1-2\cos^2\hat{y}) \frac{x^4}{3} P(x)dx$$

$$= \alpha^2 \langle x^2 \rangle + \frac{1}{3} \alpha^4 (1-2\cos^2\hat{y}) \langle x^4 \rangle$$

Now noting that $|1-2\cos^2\hat{y}| \leq 1$, and assuming that the second and fourth moments of x exist, one has for sufficiently small α:

$$\sin^2(\alpha x) \cong \alpha^2 \langle x^2 \rangle$$

Summarizing, $\langle \sin^2(\alpha x) \rangle$ approaches ½ for very large α and is proportional to α^2 for sufficiently small α. A specific example has been calculated in the text employing exponentially distributed x with mean L_0 for which one obtains

$$\langle \sin^2(\alpha x) \rangle = \frac{1}{2} \frac{(2\alpha L_0)^2}{1 + (2\alpha L_0)^2}$$

This is clearly equal to 1/2 for very large α and proportional to α^2 for small α.

BIBLIOGRAPHIC DATA SHEET

1. Report No. TM 79544	2. Government Accession No.	3. Recipient's Catalog No.
4. Title and Subtitle The Influence of Tortuosity on the Spectrum of Radiation from Lightning Return Strokes		5. Report Date 6. Performing Organization Code
7. Author(s) D. M. Le Vine		8. Performing Organization Report No.
9. Performing Organization Name and Address Microwave Sensors Branch Goddard Space Flight Center Greenbelt, Maryland 20771		10. Work Unit No. 11. Contract or Grant No. 13. Type of Report and Period Covered
12. Sponsoring Agency Name and Address Microwave Sensors Branch Goddard Space Flight Center Greenbelt, Maryland 20771		14. Sponsoring Agency Code

15. Supplementary Notes

16. Abstract

An investigation has been made of the influence of tortuosity on the spectrum of radiation from lightning return strokes. The shape of the spectrum obtained by including effects of tortuousity is in keeping with data: The spectrum has a peak in the correct frequency regime followed by an initial decrease as the inverse of frequency. This spectrum is in better agreement with data than the spectrum predicted by the same model without tortuousity (i.e. the long straight channel), which decays at a rate proportional to $1/\nu^2$.

These conclusions were derived from a piecewise-linear "transmission line" model for the channel using in one case simplifying assumptions to arrive at closed form expressions for the spectrum and also from numerical calculations on simulated channels. The analysis indicates an eventual transition to $1/\nu^2$ decrease even for the tortuous channel, which suggests a means for testing the model and gaining insight into return stroke current and channel parameters.

17. Key Words (Selected by Author(s))	18. Distribution Statement
Lightning Radiation Lightning Tortuosity Lightning Spectrum	

19. Security Classif. (of this report)	20. Security Classif. (of this page)	21. No. of Pages	22. Price*

*For sale by the National Technical Information Service, Springfield, Virginia 22151.